

## Mapping of Deletions and Substitutions in Heteroduplex DNA Molecules of Bacteriophage Lambda by Electron Microscopy

**Abstract:** Electron microscopy of heteroduplex DNA molecules, composed of one strand of *Escherichia coli* phage  $\lambda^+$  DNA annealed to the complementary DNA strand of a  $\lambda$  deletion or substitution mutant, permits visualization, as well as precise measurements and mapping, of the unpaired single-stranded regions of nonhomology in the otherwise double-stranded molecules. In the  $\lambda b2$  mutant, the central segment (13 percent) of the  $\lambda^+$  DNA molecule is shown to be deleted. In the hybrid phages  $\lambda i^{434}$  and  $\lambda i^{21}$  a segment of the right arm of the  $\lambda^+$  genome (5.5 or 7.6 to 9 percent) is replaced by the corresponding immunity regions of phage 434 (3.3 percent or phage 21 (4 percent) DNA. The  $b5$  region in the  $\lambda b5$  mutant appears to be identical to the  $i^{21}$  segment. From these data it is possible to estimate the size and position of those  $\lambda$  genes which are replaced by the  $i^{434}$  and  $i^{21}$  segments. The method permits preparing complete physical maps of viral genomes with a precision heretofore unattainable.

One of the aims of classical cytogenetics is to relate the chromosome dimensions and general morphology to the genetic maps deduced from recombination experiments. This approach has been only partially successful because of the complex and largely unknown fine structure of the chromosomes in higher organisms. The genome of the bacteriophage  $\lambda$  is much simpler, consisting of a single linear DNA molecule, which can be seen in the electron microscope. Furthermore, there are numerous mutants of  $\lambda$  readily available, in which practically any region of the genome has been deleted or replaced by nonhomologous DNA derived from the host or other phages. These may be classified into three most common types: (i) deletions within the central region of the  $\lambda$  DNA molecule, as exemplified by the  $b2$  deletion; (ii) hybrids between  $\lambda$  and  $\lambda$ -related phages, including the special case of substitutions in the immunity region, such as  $\lambda i^{434}$ ,  $\lambda i^{21}$ , and  $\lambda b5$ ; and (iii) substitutions consisting of *Escherichia coli* DNA within the left ( $\lambda dgal$ ) or right arm ( $\lambda bio$  and  $\lambda dbio$ ) of the  $\lambda$  molecule (1). The position of all these deletions can be mapped by standard genetic crosses.

We now show that very precise physical maps of these deletions can be prepared by combining electron microscopy and DNA-DNA hybridization techniques. The precision of the mapping is much higher than that for any other known method; the standard deviation is frequently less than 2 percent. The principle of the technique is as follows. The complementary DNA strands of wild-type  $\lambda$  ( $\lambda^+$ ) and of a deletion or substitution mutant are preparatively separated (2). One strand

of  $\lambda^+$  DNA is hybridized with the complementary strand derived from the mutant strain DNA. The resulting heteroduplex is a double-stranded molecule with the exception of the regions of nonhomology. For a simple deletion, such as that of region  $b2^+$ , the heteroduplex between the  $\lambda^+$  and  $\lambda b2$  strands of DNA should appear as an uninterrupted double-stranded molecule of  $\lambda b2$  length with a single-stranded loop formed from the unpaired segment of the  $\lambda^+$  strand, as schematically depicted in Fig. 1. On the other hand, substitution by a nonhomologous region in one strand of the heteroduplex should be seen as a stretch of two unpaired single DNA strands (such as region  $i^{\lambda}/i^{21}$  in Fig. 1) bridging a gap between the double-stranded regions. These predictions were fully confirmed by preparing electron micrographs of heteroduplex molecules in which the single-stranded DNA segments are well extended and could be readily identified and measured; their exact position was accurately determined with respect

to the termini of the molecule and to other single-stranded regions (see Figs. 3 to 5). Independently, Davis and Davidson (3) have used a somewhat similar approach, although the single DNA strands were collapsed ("bushes") in their electron microscopic preparations; thus, they were unable to determine the length and fine structure of the unpaired single-stranded regions. They did not fractionate the complementary DNA strands, and their method of renaturation of the mixture of denatured DNA's differed from ours.

The separated  $l$  and  $r$  DNA strands of  $\lambda c_{72}$ ,  $\lambda cb2$ ,  $\lambda cb2b5$ ,  $\lambda i^{434}$ ,  $\lambda i^{21}$  and  $\lambda b2i^{21}$  (1) were isolated as described by Hradecna and Szybalski (2), with the use of equilibrium centrifugation in CsCl gradients containing poly(U,G), a copolymer of guanylic and uridylic acids. Heteroduplexes were prepared by the following procedure, adapted from Subirana (4). To 1 ml of 50 percent formamide solution (1 volume of formamide and 1 volume of 0.01M NaHCO<sub>3</sub>, pH 8.6) was added 10  $\mu$ l from each of two freshly prepared 6M CsCl gradient fractions, one containing the separated strands  $l$  or  $r$  of  $\lambda$  DNA and the other containing the complementary strands of mutant  $\lambda$  DNA. In a similar manner, homoduplex controls were prepared. The final concentrations were 1 to 4  $\mu$ g of DNA per milliliter of 0.12M CsCl. Annealing was carried out at 4°C for 5 days or longer.

The DNA was prepared for electron microscopy by a modification of the basic-protein film technique of Kleinschmidt and Zahn (5). The cytochrome *c* solution was filtered through 0.2- $\mu$  Flotronics membranes (FM-13; Selas), whereas all other solutions were filtered

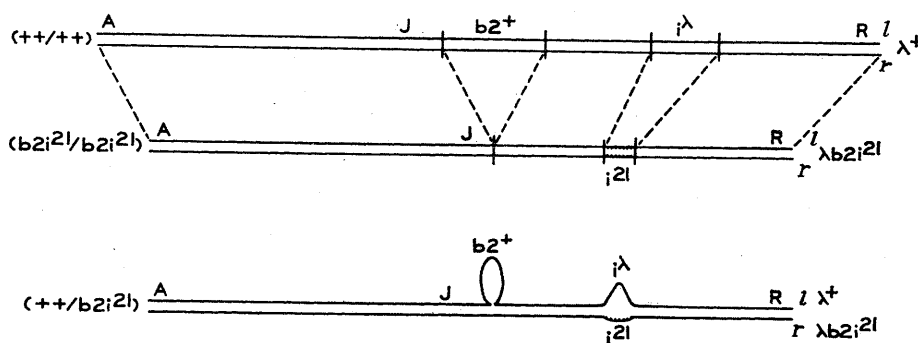


Fig. 1. Representation of a heteroduplex DNA molecule ( $+/+/b2i^{21}$ ; bottom drawing) formed by annealing the  $l$  strand ( $+/+$ ) of  $\lambda^+$  with the  $r$  strand ( $b2i^{21}$ ) of  $\lambda b2i^{21}$  (1). The corresponding homoduplexes are represented by the two upper diagrams. In  $\lambda b2i^{21}$  the  $b2^+$  region is deleted, whereas region  $i^{\lambda}$  is replaced by a shorter nonhomologous region  $i^{21}$  (knobby line).

through 0.22- $\mu$  Millipore membranes to eliminate the particulate matter, which contributes to the clumping of the DNA molecules. A mixture composed of 0.1 ml of the DNA solution in 50 percent formamide and 0.01 ml of 0.1 percent cytochrome c (Nutritional Biochemicals) was spread on a surface of twice-distilled water from an inclined, acid-cleaned, glass slide. The monolayer containing DNA was then transferred to specimen grids and dehydrated for 5 seconds each in absolute ethanol, amyl acetate, and 2-methylbutane. The most satisfactory results were obtained with platinum specimen grids (19 drilled holes; Siemens America) coated with Formvar membranes. A fresh solution of 0.3 percent Formvar (Shawinigan Resins) in 1,2-dichloroethane was dried on a glass cover slip. The film was then cast onto distilled water in a sintered-glass funnel and drawn down onto platinum specimen grids, lightly coated with carbon, and used the same day.

The DNA was rendered visible by shadow-casting with uranium oxide. Approximately half of the nitrocellulose binder was removed from commercial uranium oxide (E. F. Fullam) by extracting with acetone, discarding half of the supernatant from the sediment, and evaporating the solvent remaining with the uranium oxide sediment, while mixing to obtain an even distribution of binder. This uranium oxide (12 mg) was evaporated from a tungsten wire basket at an angle of 6° to 7°, with a distance of 11 cm between the basket and rotating specimen (10 rev/min). The nitrocellulose was first removed by slowly heating at a pressure less than 0.1  $\mu$ -Hg. The uranium oxide was evaporated by rapid heating for 5 to 10 seconds at a pressure lower than 0.03  $\mu$ -Hg (Kinney evaporator SC-3 with a liquid nitrogen trap).

Electron micrographs (Kodak electron image plates) were taken with a Siemens Elmiskop I (intermediate lens off, projector polepiece III, double condenser illumination, 10,700 $\times$ , 60 kv, 15- $\mu$  objective aperture). Magnification was calibrated with a carbon replica of a diffraction grating (54,864 lines per inch; E. F. Fullam). The DNA molecules were measured as described by Ris and Chandler (6). To minimize variation in magnification all the micrographs from one grid were taken without realigning the microscope or repositioning the grid. The illuminated area on the viewing screen was ad-

Table 1. Length comparisons between homoduplexes or homoduplex regions of DNA. Each set of two was placed on the same grid.

Homoduplex (or homoduplex region)	Length ( $\mu$ )	Standard deviation* (%)
$\lambda b2/\lambda b2$	14.8	1.6
$\lambda^+/\lambda^+$	17.0	0.9
$\lambda b2/\lambda b2$	14.8	2.1
$\lambda b2/\lambda^+$	14.7	1.5
$\lambda b2b5/\lambda b2b5$	14.2	1.2
$\lambda^+/\lambda^+$	17.0	1.4
$\lambda^{i44}/\lambda^{i44}$	16.6	2.1
$\lambda b2/\lambda^+$	14.8	2.0

\* Percent of indicated length, for example, 14.8  $\pm$  0.24 (1.6 percent).

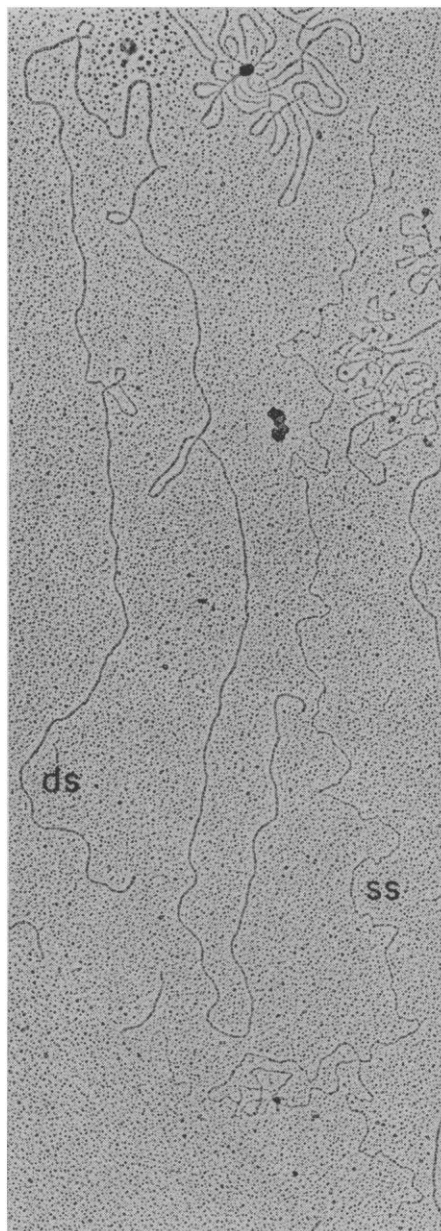


Fig. 2. Electron micrograph of a double-stranded (ds) homoduplex of  $\lambda^+$  DNA, prepared by annealing the separated *l* and *r* strands, and of an unpaired single-stranded  $\lambda^+$  DNA molecule (ss).

justed to the same size before each photograph. One hour was allowed after the lenses were turned on before the micrographs were taken, and the lenses were turned off and on several times to reduce hysteresis. Where comparison of the lengths of two different molecules was needed, a mixture of both duplexes was placed on the same grid. Each value represents 20 to 40 measurements on nonambiguous configurations. The standard deviations were about 2 percent for double-stranded DNA and about 5 percent for single-stranded DNA.

As evident in Fig. 2, the annealing of two complementary strands of  $\lambda$  DNA results in the formation of uniformly double-stranded homoduplexes (ds). The number of such duplexes formed depends on the time allowed for annealing (80 percent after 2 weeks). Some circular duplexes (6) (Fig. 4A) were present in all preparations, an indication that the conditions of annealing permit pairing of homologous terminal regions of  $\lambda$  as short as only 20 base pairs. Under the described conditions of annealing, spreading, and shadowing, the homoduplexes (ds) appear somewhat thicker and more rigid than the single DNA strands (ss), an example of which also appears in Fig. 2. Moreover, the single strands, although somewhat kinky in appearance, are reasonably well extended, although their length is variable, being frequently 5 to 10 percent longer than the corresponding double strands (Tables 1 and 2). Thus, by this technique double-stranded and single-stranded molecules can be easily distinguished.

Heteroduplexes ( $+/b2b5$ ) composed of an *l* strand of  $\lambda^+$  DNA ( $++$ ) and an *r* strand of  $\lambda b2b5$  ( $b2b5$ ) are shown in Fig. 3, A-D. The molecules appear double-stranded except for two regions: a single-stranded loop ( $b2^+$ ), which must correspond to the  $b2^+$  region comprising the central sector (13 percent) of the  $\lambda^+$  strand and deleted in the  $\lambda b2$  mutant (7), and an unpaired region with one single-stranded segment longer than the other. An enlargement of a  $b2^+$  loop is shown in Fig. 3C. As expected for a simple deletion (Fig. 1), no apparent interruption in the double-stranded configuration occurs at the point where the single-stranded loop emanates from the double helix (Fig. 3, A-C). Figure 3D shows in greater detail the  $b5/i\lambda$  ( $b5^+/+$ ) nonhomology region. It is obvious from this micrograph and Fig.

3A that there is a discontinuity in the double-stranded structure, which bifurcates into two single-stranded regions before rejoining. The shorter single-stranded segment must correspond to the b5 region, since the  $\lambda b5$  (b5/b5) DNA molecule is shorter than  $\lambda^+$  (+1+) DNA (1, 2, 7 and Tables 1, 2, and 3). Practically identical results, well within the standard experimental error (Table 2), were obtained when one strand of the heteroduplex was de-

rived from  $\lambda^+$  and the other from the  $\lambda b2i^{21}$  hybrid, in which the  $\lambda$  genes N, *rex*, *c<sub>I</sub>*, *x*, *y*, and *c<sub>II</sub>* have been replaced by the analogous segment of the phage 21 genome (1, 8, 9, 10). This similarity suggests that the *i<sup>21</sup>* region is identical with the b5 region. More recently, corroboration of this notion has been provided by studies carried out in cooperation with Dr. Z. Hradecna, in which it was shown that heteroduplexes between  $\lambda b2b5$  and  $\lambda b2i^{21}$

appear as perfectly double-stranded molecules, free of any readily discernible single-stranded regions.

Another example of an unpaired single-stranded region is provided by a heteroduplex between strand *l* of  $\lambda b2$  and strand *r* of  $\lambda i^{434}$  (7, 11). In the latter phage,  $\lambda$  genes *rex*, *c<sub>I</sub>*, and *x* have been replaced by a corresponding but somewhat shorter segment [as judged by buoyant density data and length measurements; see (1) and Tables 1, 2,

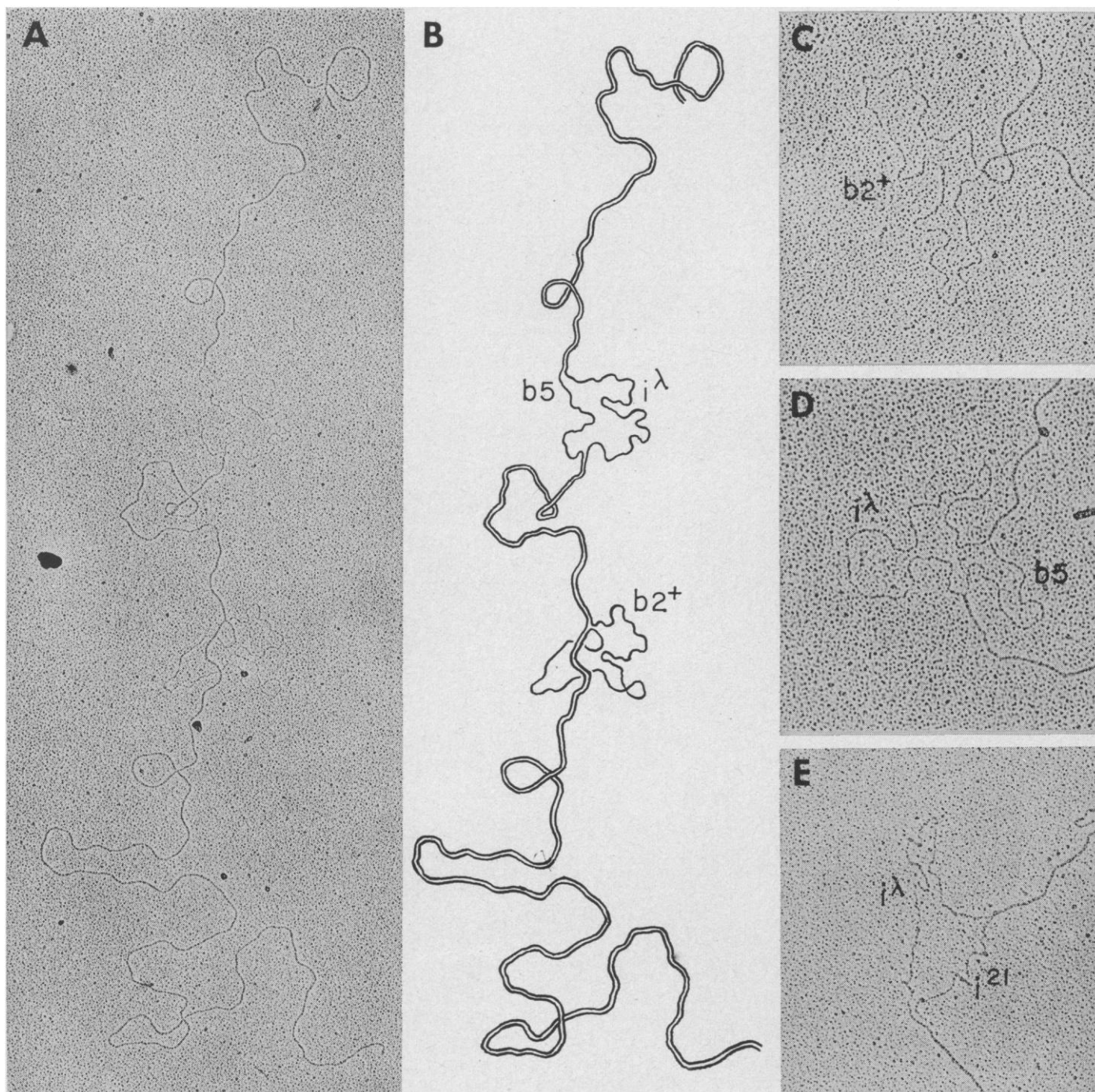


Fig. 3. Electron micrographs of heteroduplex  $\lambda$  DNA molecules. (A) Heteroduplex between strand *l* of  $\lambda^+$  and strand *r* of  $\lambda b2b5$  (++/b2b5). (B) An interpretive drawing of the ++/b2b5 heteroduplex, including the single-stranded  $b2^+$  loop and the unpaired segment  $i^\lambda/b5$  (+/b5). (C) Enlargement of another  $b2^+$  loop. (D) Enlargement of another  $i^\lambda/b5$  (+/b5) unpaired region. (E) Enlargement of the  $i^\lambda/i^{21}$  (+/ $i^{21}$ ) unpaired region.

Table 2. Length of single-stranded (ss) and double-stranded (ds) regions in heteroduplexes of  $\lambda$  DNA.

Segment of $\lambda$	Length ( $\mu$ )	S.D.* (%)	Length (% of $\lambda^+$ )
$\lambda^{i^{434}}/\lambda b2$			
Left $\lambda$ terminus to $b2^+$ loop (ds)	7.53	2.3	44.3
$b2^+$ loop (ss)	2.33	5.9	13.0 $\dagger$
$b2^+$ loop to left bifurcation of $i^{434}/i^{\lambda}$ (ds)	2.78	4.3	16.3
$i^{\lambda}$ (ss)	0.99	5.1	5.5 $\dagger$
$i^{434}$ (ss)	0.58	4.6	3.3 $\dagger$
Right bifurcation of $i^{434}/i^{\lambda}$ to right $\lambda$ terminus (ds)	3.54	2.9	20.9
$\lambda b2b5/\lambda^+$			
Left $\lambda$ terminus to $b2^+$ loop (ds)	7.53	1.9	44.3
$b2^+$ loop (ss)	2.48	5.9	13.0 $\dagger$
$b2^+$ loop to left bifurcation of $b5/i^{\lambda}$ (ds)	2.30	7.3	13.5
$i^{\lambda}$ (ss)	1.71	3.4	9.0 $\dagger$
$b5$ (ss)	0.76	5.5	4.0 $\dagger$
Right bifurcation of $b5/i^{\lambda}$ to right $\lambda$ terminus (ds)	3.43	1.8	20.2
$\lambda b2i^{21}/\lambda^+\ddagger$			
Left $\lambda$ terminus to $b2^+$ loop (ds)	7.53	4.5	44.3
$b2^+$ loop (ss)	1.78	17.2	13 $\dagger$
$b2^+$ loop to left bifurcation of $i^{21}/i^{\lambda}$ (ds)	2.37	9.4	13.8
$i^{\lambda}$ (ss)	1.17	11.5	8.4 $\dagger$
$i^{21}$ (ss)	0.62	13.6	4.4 $\dagger$
Right bifurcation of $i^{21}/i^{\lambda}$ to right $\lambda$ terminus (ds)	3.52	4.9	20.5

\* Percent standard deviation for each region, for example,  $7.53 \pm 0.17$  (2.3 percent).  $\dagger$  Corrected to equivalent of double-stranded length, taking the  $b2^+$  loop as equal to 13 percent of the  $\lambda^+$  length.  $\ddagger$  Preliminary measurements for 20 heteroduplex molecules, with the distance from the left  $\lambda$  terminus to the  $b2^+$  loop used as a standard (7.53  $\mu$ ).

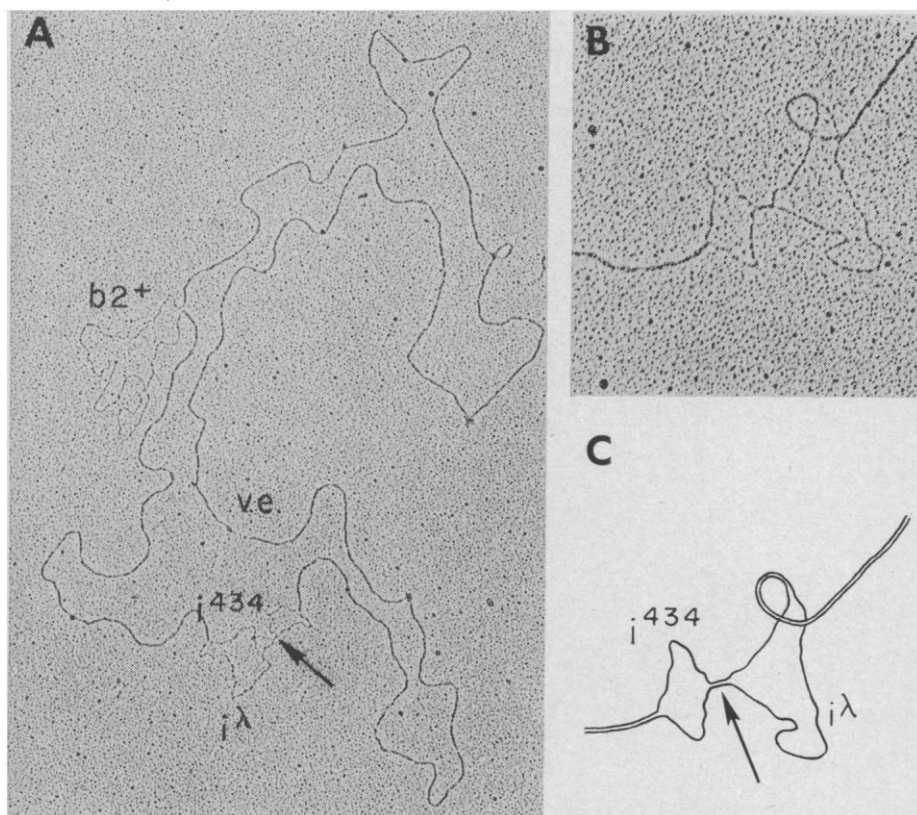


Fig. 4. Electron micrographs of heteroduplex molecules between the  $l$  strand of  $\lambda b2$  and the  $r$  strand of  $\lambda^{i^{434}}$  DNA. (A) Intact circular heteroduplex molecule. It appears that, due to tensions generated during drying of the DNA heteroduplex on the Formvar film, the vegetative (cohesive) ends (*v.e.*) have become disengaged and the  $l$  strand of the  $\lambda b2$  DNA has broken at the point where the single-stranded  $b2^+$  loop emerges. (B) Enlargement of another unpaired segment  $i^{\lambda}/i^{434}$ , and its interpretative drawing (C).

and 3] carrying the immunity region  $i^{434}$  of phage 434 (8, 9, 11). As shown in Figs. 4 and 5, the region of non-homology between  $\lambda^{i^{434}}$  and  $\lambda^+$  is shorter than that observed for the  $i^{21}$  or  $b5$  substitutions. A further complexity, which was not observed in the  $b5/+$  or  $i^{21}/+$  nonhomology regions, is indicated by the arrows in Fig. 4. In most of the unpaired  $i^{434}/i^{\lambda}$  regions the single strands meet (pair?) at a specific location (Fig. 5B). This probable homology region corresponds to less than 0.3 percent (150 base pairs) of the  $\lambda^+$  DNA length but may actually be much shorter, since homologies consisting of only 20 nucleotides can be visualized by our technique, as pointed out for circular  $\lambda$  molecules.

Our results have been compared with molecular and genetic data obtained by other investigators using different or similar approaches. The figure of 13 percent, representing the length of the  $b2$  deletion, compares favorably with recent sedimentation data which indicate that 13.6 percent of  $\lambda^+$  DNA is deleted in the  $\lambda b2$  mutant (12). These figures are somewhat lower than those reported earlier and summarized in Table 3. The only lower value (11.2 percent) for the length of the  $b2$  deletion was computed indirectly by comparing the electron micrographic lengths of  $\lambda^+$ ,  $\lambda b2b5$ , and  $\lambda b5$  DNA (3), although more recent measurements performed in the same laboratory indicate a  $b2^+$  length of 12.6 percent (13). On the basis of genetic data (14) and the nucleotide distribution in  $\lambda^+$  and  $+\lambda b2$  DNA (15), it was previously concluded that the  $b2^+$  region occupies the central portion of the  $\lambda^+$  DNA molecule. In our micrographs of the  $b2/+$  heteroduplex the  $b2^+$  loop emanates at a point 50.8 percent from the left and 49.2 percent from the right end of the double-stranded structure. There is less than 1 percent difference between this result and other electron micrographic measurements (3, 13).

The immunity region of  $\lambda$ , which is within the unpaired segments  $i^{434}/+$ , and  $i^{21}/+$  (1, 8-11), is located near the middle of the right arm of the  $\lambda^+$  DNA molecule. Comparison of the electron micrographic measurements (Fig. 5, A and B) with the genetic data permits assignment of lengths and positions to the  $\lambda$  genes located within the region replaced by the  $i^{434}$  and  $i^{21}$  segments and in their immediate vicinity. The approximate position of the left end of gene N, as based on the sedimentation data for infectious DNA

fragments [73 percent from the left  $\lambda^+$  terminus (16)] agrees well with its placement between the left ends of the  $i^{434}$  and  $i^{21}$  substitution and with our measurements of the respective distances from the left terminus amounting to 73.6 percent and 70.8 to 72.2 percent of the  $\lambda^+$  molecule (16a). The distance measured between the left ends of the  $i^{21}$  and  $i^{434}$  substitutions permits assignment of 1.4 to 2.8 percent (see 16a) to that region of the  $\lambda$  genome which contains mutations *sus7* and *sus53* (see 9, 17) in gene N (Fig. 5C). However, the size of that portion of gene N which lies between the  $i^{21}$  and  $i^{434}$  substitutions appears much smaller, when one compares the difference in length between heterologous regions  $i^{21}$  and  $i^{434}$ , which is only 0.7 percent of the  $\lambda^+$  length. To make the latter comparison, one must assume that the gene supplied by phage 21 in the  $\lambda i^{21}$  hybrid corresponds to gene N of  $\lambda$ , both in function and in length. Since the only known difference between the  $i^{21}$  and  $i^\lambda$  regions is the absence of the *rex* function, the length of the  $i^{21}$  substitution (4 percent of the  $\lambda^+$  length) must accommodate the functions corresponding to the following  $\lambda$  genes and controlling elements: N, promoter ( $p_L$ ) and operator ( $o_L$ ) for the N operon, repressor gene  $c_I$ , promoter ( $p_R$ ) and operator ( $o_R$ ) for the *x-O-P* operon, regions *x* and *y*, and gene  $c_{II}$  (1, 9, 10, 17).

Gene  $c_I$ , whose length should correspond to approximately 2 percent of the  $\lambda^+$  DNA molecule, as judged from the molecular weight of the  $c_I$  protein (18), should be located to the right of gene *rex* within the region defined by the  $i^{434}$  substitution (Fig. 5C). This result, which places the right end of  $c_I$  at least 76 percent from the left  $\lambda^+$  terminus, indicates that the  $\lambda$  region which is characterized by 43 percent guanine + cytosine (G+C) content must extend more than 5 percent beyond its assigned 71 percent right boundary (15), because  $c_I$ -specific messenger RNA hybridizes with those DNA fragments which contain 43 percent G+C (19).

The size of the  $\lambda$  immunity region, as defined by the  $i^{434}$  substitution, is 5.5 percent of the  $\lambda^+$  DNA length, which should be ample for genes  $c_I$  (2 percent) and *rex*, together with the two  $c_I$ -controlled operators,  $o_L$  (left) and  $o_R$  (right), the latter in region *x* (8, 17, 18). The analogous functions, with the exception of gene *rex*, must occupy only 3.3 percent in phage 434

Table 3. Various estimates of the net loss in the  $\lambda^+$  DNA length (percent) as a result of the b2 deletion and the b5,  $i^{21}$  and  $i^{434}$  substitutions.

Measurement	Phage						Reference
	$\lambda^+$	$\lambda b2$	$\lambda i^{434}$	$\lambda i^{21}$	$\lambda b5$	$\lambda b2i^{21}$	
<i>Electron microscopy</i>							
Percent deleted	0						23 (23)
Percent deleted	0	17.8					(24)
Percent deleted	0	(11.2)*			5.3		16.5 (3)
Percent deleted	0	13.0	2.2†	4.0†	5.0†		16.5 (Present data) (16a)
				3.6†	3.5*		
<i>Density of heterodimers</i>							
Percent deleted	0	15.3					(25)
<i>Zone sedimentation</i>							
Percent deleted	0	15.1			7.5		19.0-20.7 (26)
Percent deleted	0	13.6					(12)
<i>Buoyant density of phage in CsCl gradient</i>							
Percent deleted	0	14.7	2.8	5.9	5.9	20.5	20.5 (1, 2)‡
Density (g/cm <sup>3</sup> )	1.508	1.491	1.505	1.501 <sub>s</sub>	1.501 <sub>s</sub>	1.483 <sub>s</sub>	1.483 <sub>s</sub>
Percent deleted	0	14.7			6.4		20.9 (7)‡
Density (g/cm <sup>3</sup> )	1.508	1.491			1.501		1.483
Percent deleted	0				5.5		17.9 (3)‡
Density (g/cm <sup>3</sup> )	1.508				1.502		1.487

\* Value obtained indirectly from the difference between measurements of double-stranded DNA.  
 † Difference between the lengths of the single DNA strands in unpaired regions (corrected to equivalent of double-stranded length).  
 ‡ Percent deleted was calculated (or presently recalculated from the formula in (3).

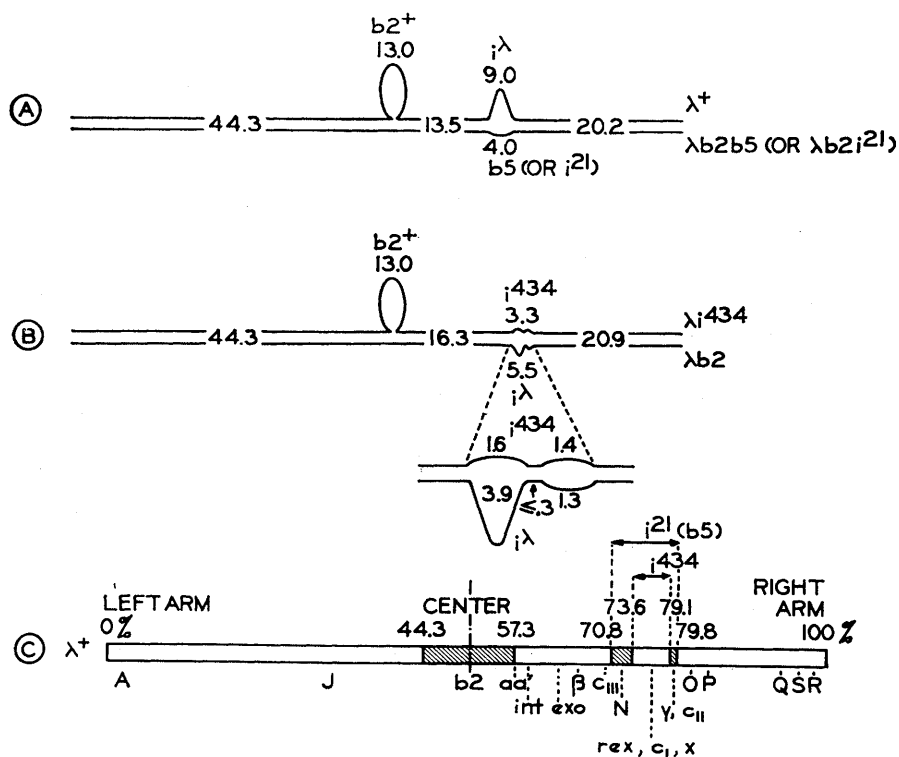


Fig. 5. Representation of heteroduplex  $\lambda$  DNA molecules and the physical map of  $\lambda^+$  DNA derived from measurements of the double-stranded and unpaired regions in the heteroduplexes. (A) Linear dimensions of a heteroduplex formed by annealing one strand of  $\lambda^+$  with the complementary strand of  $\lambda b2b5$ . Practically identical results were obtained when one strand of  $\lambda^+$  was annealed with the complementary strand of  $\lambda b2i^{21}$  DNA (Fig. 3E and Table 2; see also 16a). (B) Linear dimensions of a heteroduplex formed by annealing of one strand of  $\lambda i^{434}$  with the complementary strand of  $\lambda b2$ . The enlarged section of the map represents the fine structure of the unpaired  $i^\lambda/i^{434}$  region including the short segment of apparent homology. (C) Physical map of  $\lambda^+$  DNA with the position of the deleted or substituted regions indicated as the distance from the left terminus, expressed in percent of the total length of the  $\lambda^+$  DNA molecule. The location of the various genes is indicated on this physical map. Site  $aa'$  (57.3 percent) is the crossover point between  $\lambda$  and *E. coli* DNA in *int*-mediated  $\lambda$  integration or excision (16a, 17). [For a description of the genes see (2, 8, 9, 17); for more recent measurements of the position of the left end of the  $i^{21}$  substitution (72.2 percent instead of 70.8 percent) see (16a).]

and less than 4 percent in phage 21. The  $c_I$  gene of  $\lambda$  should be similar in size to the repressor gene of phage 434, since the molecular weights are similar (20). At present it is difficult to speculate on the meaning of the short region of apparent homology within the unpaired  $i^{434}/+$  segment, probably within gene  $c_I$  (Fig. 5B).

The distance between the right ends of the  $i^{434}$  and  $i^{21}$  substitutions permits assignment of 0.7 percent of the  $\lambda^+$  length to region  $y$  and gene  $c_{II}$ . There is excellent agreement between the earlier mapping of the left end of gene O [79 to 81 percent from the left terminus (16)] and the position of the right end of the  $i^{21}$  substitution (79.8 percent from the left terminus), which is located between genes  $c_{II}$  and O (Fig. 5C).

Another conclusion to be derived from our data is the identity or near identity of the so-called b5 region in the  $\lambda b5$  "mutant" and the  $i^{21}$  non-homology region in  $\lambda i^{21}$  (1, 7). Phage  $\lambda b5$ , which has a density identical to that of phage  $\lambda i^{21}$  and which has the immunity of phage 21 (1, 7, 21), is a recombinant between  $\lambda^+$  and the descendants of a plaque which appeared as a fortuitous contaminant during crossing of  $\lambda$  mutants (22). Our data on the position of the b5 region agree well with the results of Davis and Davidson (3), although the length computed by them for the corresponding deletion in the  $\lambda$  genome is substantially lower (5.3 percent) than the value we obtained by direct measurement of the homoduplexes (Table 1 and 3) and the single-stranded  $\lambda$  DNA [7.6 to 9 percent (16a)] within the unpaired b5/+ region (Fig. 5A).

The lack of pairing between particular regions of the  $l$  and  $r$  strands in a heteroduplex could be caused either by substitution or by inversion of a segment of the genome. In the case of inversion, the base sequences of the single DNA strands in the unpaired region would be identical instead of complementary. The differences in length between the single-stranded  $i^{\lambda}$  segment on one hand, and the corresponding  $i^{434}$ ,  $i^{21}$ , or b5 segments on the other, provide an argument against inversion; the absence of any observable homologies between the  $r$  strands of  $\lambda^+$  and the  $r$  strands of the  $\lambda b5$  mutant is also an argument against inversion.

It can be concluded that the method described, whereby both the single-stranded and double-stranded regions

of various heteroduplexes of viral DNA can be accurately measured, permits the construction of precise molecular maps, including the assignment of both position and size to various genes (28).

BARBARA C. WESTMORELAND

WACLAW SZYBALSKI, HANS RIS

Department of Zoology and McArdle Laboratory, University of Wisconsin, Madison 53706

#### References and Notes

- The strains used are listed in Ref. 2. Phage  $\lambda c_{72}$  will be referred to as  $\lambda^+$  or (+) in our report, since the electron microscopic appearance of  $\lambda c_{72}$  DNA is indistinguishable from that of the parental ("wild type") strain  $\lambda_{PAPA}$  (9-11), from which it differs by a point mutation in gene  $c_I$ . In phages  $\lambda b2$  and  $\lambda b2$ , the central  $b2^+$  region has been deleted (7), whereas the symbols  $i^{21}$  and  $i^{434}$  indicate that a segment of the  $\lambda$  genome, including the so-called immunity region  $i^{\lambda}$ , has been deleted and replaced by analogous regions of the  $\lambda$ -related phages 21 or 434, respectively. Strains  $\lambda i^{434}$  and  $\lambda i^{21}$  were originally described as 434hy and 21hy1, respectively (10, 11). As evident in this communication and from immunity studies (9, 21, 22), region b5 in phages  $\lambda b5$  or  $\lambda b2b5$  (7) is probably identical to  $i^{21}$ . The buoyant densities of these phages, as measured by Hradecna and Szybalski (2), are 1.508 g/cm ( $\lambda c_{72}$  or  $\lambda_{PAPA}$ ), 1.491 ( $\lambda b2$  or  $\lambda b2b5$ ), 1.483 to 1.484 ( $\lambda b2b5$ ), 1.505 ( $\lambda i^{434}$ ), 1.501 ( $\lambda i^{21}$ ), and 1.483 to 1.484 ( $\lambda b2i^{21}$ ); see also Table 1. The symbols  $\lambda dgal$ ,  $\lambda bio$ , and  $\lambda dbio$  designate defective ( $d$ ) or plaque-forming phages in which some  $\lambda$  genes were replaced by *E. coli* DNA (9, 27). For definition of DNA strands  $l(=W)$  and  $r(=C)$  see (2) and (17).
- Z. Hradecna and W. Szybalski, *Virology* **32**, 633 (1967); unpublished data.
- R. W. Davis and N. Davidson, *Proc. Nat. Acad. Sci. U.S.A.* **60**, 243 (1968).
- J. A. Subirana, *Biopolymers* **4**, 189 (1965).
- A. K. Kleinschmidt and R. K. Zahn, *Z. Naturforsch.* **14b**, 770 (1959).
- H. Ris and B. L. Chandler, *Cold Spring Harbor Symp. Quant. Biol.* **28**, 1 (1963).
- G. Kellenberger, M. L. Zichichi, J. Weigle, *Nature* **187**, 161 (1960).
- H. A. Eisen, C. R. Fuerst, L. Siminovich, R. Thomas, L. Lambert, L. Pereira Da Silva, F. Jacob, *Virology* **30**, 224 (1966);  $\lambda$  genes N and  $c_{II}$  are also deleted in phage  $\lambda b5$  (W. F. Dove, personal communication).
- W. F. Dove, *Ann. Rev. Gen.* **2**, 305 (1968).
- M. Liedtke-Kulke and A. D. Kaiser, *Virology* **32**, 475 (1967).
- A. D. Kaiser, *ibid.* **3**, 42 (1957); ——— and F. Jacob, *ibid.* **4**, 509 (1957).
- E. Burgi, personal communication.
- J. S. Parkinson and R. W. Davis, personal communication.
- E. Jordan, *J. Mol. Biol.* **10**, 341 (1964).
- A. Skalka, E. Burgi, A. D. Hershey, *ibid.* **34**, 1 (1968).
- D. S. Hogness, W. Doerfler, J. B. Egan, L. W. Black, *Cold Spring Harbor Symp. Quant. Biol.* **31**, 129 (1966).
- 16a. Recent electron micrographic measurements of heteroduplexes formed between  $l$  strands of  $\lambda i^{21}$  and  $\lambda i^{434}$  DNA and  $r$  strands of  $\lambda bio$  phages (1), in which most of the  $\lambda$  DNA between the right end of  $b2^+$  and the left end of the  $i^{21}$  region has been replaced by *E. coli* DNA, indicate that the left end of the  $i^{21}$  substitution is located 72.2 percent from the left  $\lambda^+$  terminus—that is, 1.4 percent farther to the right than the distance of 70.8 percent shown in Fig. 5c (Z. Hradecna and W. Szybalski, *Virology*, in press; D. M. Zuhse, M. J. Fiantz, Z. Hradecna, W. Szybalski, unpublished). The  $i^{\lambda}$  region in the  $\lambda^+/\lambda b2i^{21}$  heteroduplex (Fig. 5A) thus would have to be shortened to 7.6 percent of the  $\lambda^+$  length. The difference between the lengths of the  $i^{\lambda}$  and  $i^{21}$  regions would then become 3.6 percent (7.6 minus 4.0), which value is in excellent agreement with the computed difference of 3.5 percent between

- the total lengths of the  $\lambda b2/\lambda b2$  and  $\lambda b2b5/\lambda b2b5$  homoduplexes [ $100 \times (14.8 - 14.2)/17.0 = 3.5$ ; Tables 1 and 3]. Other measurements summarized in Fig. 5C remain unaltered by the aforementioned recent studies.
- W. Szybalski, *Can. Cancer Conf.*, in press.
  - M. Ptashne, *Nature* **214**, 232 (1967); ——— and N. Hopkins, *Proc. Nat. Acad. Sci. U.S.A.* **60**, 1282 (1968); mutation  $v_2$  identifies the  $o_L$  operator and mutations  $v_1, v_3$  identify the  $o_R$  operator (17).
  - P. D. Bear and A. Skalka, *Carnegie Inst. Wash. Year B.* **67**, 557 (1968); personal communication.
  - V. Pirrotta, personal communication.
  - S. Brenner, personal communication.
  - J. Weigle, personal communication.
  - L. A. MacHattie and C. A. Thomas, Jr., *Science* **144**, 1142 (1964).
  - L. G. Caro, *Virology* **25**, 226 (1965).
  - R. L. Baldwin, P. Barrand, A. Fritsch, D. A. Goldthwait, F. Jacob, *J. Mol. Biol.* **17**, 343 (1966).
  - E. Burgi, *Proc. Nat. Acad. Sci. U.S.A.* **49**, 151 (1963).
  - B. Westmoreland, thesis, University of Wisconsin (1968).
  - Supported in part by NSF grants RG4738 and GB-2096 and by NIH grant GM 4738. We thank Drs. Z. Hradecna and A. Guha for the separated strands of  $\lambda$  DNA and Miss Elaine C. Babitz for measuring the contour length of the DNA molecules. We also thank Drs. J. Weigle, N. Davidson, and A. D. Hershey for helpful information and for reading this manuscript. Dr. N. Davidson pointed out to us that, in 1961, M. Nomura and S. Benzer [*J. Mol. Biol.* **3**, 684 (1961)] proposed the mapping of deletions by the electron microscopy of heteroduplexes, whereas our study was initiated only in 1962 by B.W. (27).

2 December 1968

### Ontogeny of Soluble and Mitochondrial Tyrosine Aminotransferases

**Abstract.** *The development of the soluble and mitochondrial forms of tyrosine aminotransferase was observed in fetal and neonatal rhesus monkey tissues. The mitochondrial activity is detectable in early fetal life; the soluble form reaches significant activity just before the birth of the animal.*

The mitochondrial form of tyrosine aminotransferase (E.C. 2.6.1.5) (TAT) which differs from the soluble form of this enzyme (1) was first detected in a liver biopsy from a patient with tyrosinemia who lacks the soluble enzyme (2). Mitochondrial TAT activity has been found in most of the tissues examined from adult rats, goats, monkeys, and humans. Because the transitory tyrosinemia observed in 89 percent of premature infants (3) has been attributed in part to low amounts of this enzyme (4), we investigated the time of appearance and development of both the soluble and mitochondrial forms. The results suggest that the control of tyrosine metabolism in the mammalian fetus may closely resemble that of the